International Journal of Bifurcation and Chaos, Vol. 13, No. 1 (2003) 251–260

STRANGE NONCHAOTIC ATTRACTOR IN HIGH-DIMENSIONAL NEURAL SYSTEM

J. W. SHUAI* and D. M. DURAND†
Department of Biomedical Engineering, Case Western Reserve University, Cleveland, OH 44106, USA
**shuai@helios.phy.ohiou.edu*
†dxd6@po.cwru.edu

Received July 11, 2001; Revised November 5, 2001

A general method for the creation of strange nonchaotic attractor is proposed. As an example, the strange nonchaotic attractor in a high-dimensional globally coupled neural system is studied numerically. For such an attractor, the time interval of continuously positive finite-time Lyapunov exponent must be smaller than the period of the driving stimulus, although it has a long-time positive tail. The intermittency between laminar and burst behavior is a characteristic dynamic of the strange nonchaotic attractors. Simulation results show that the chaotic phase occurs only within a small region around the origin in the parameter space. More than half of the large nonchaotic region is the strange nonchaotic phase. The chaotic phase is typically surrounded by strange nonchaotic attractors. This result also suggests that some biological signals that have a strange structure may be nonchaotic rather than chaotic.

Keywords: Chaos; fractal; spatiotemporal system; neural networks; EEG.

1. Introduction

The dynamical properties of spatially extended nonlinear systems such as neural networks, multimode lasers and charge-density waves have attracted great interest in the past decade. Such systems can be described by a set of coupled differential equations or iterated maps. The neural networks models and the coupled map lattices characterized by discrete space and time variables are two simple, computationally tractable dynamical systems that display behaviors qualitatively similar to those of more complicated models [Hopfield, 1982; Kaneko, 1990]. Rich spatiotemporal complex behaviors including chaos, patterns, traveling waves, memory and synchronization are revealed in such systems. Often, highly complex behavior appears in chaotic spatiotemporal systems. However, with the study of the unidirectional coupling map lattices, it has been shown that complex phenomena can also take place in some nonchaotic spatiotemporal systems [Vergni *et al.*, 1997].

A type of complex behavior occurring in nonchaotic systems is strange nonchaotic attractor (SNA) that is geometrically complicated but which trajectory does not exhibit sensitive dependence on initial conditions asymptotically [Grebogi *et al.*, 1984; Ding *et al.*, 1989; Ditto *et al.*, 1990]. Different mechanisms for the creation of SNA have been proposed in low-dimensional quasiperiodically forced systems [Heagy & Hammel, 1994; Nishikava

*Author for correspondence. Current address: Department of Physics and Astronomy, Ohio University, Athens, OH 45701-2979.

& Kaneko, 1996; Yalcinkaya & Lai, 1996; Prasad *et al.*, 1997; Brown & Chua, 1998; Shuai & Wong, 1998, 1999]. An interesting question is whether the mechanism discussed for the emergence of SNA in low-dimensional systems can be generalized to high-dimensional systems. Most of the SNA dynamics involve a collision between a stable and an unstable invariant region [Heagy & Hammel, 1994; Nishikava & Kaneko, 1996; Yalcinkaya & Lai, 1996; Prasad *et al.*, 1997]. In fact, the system often becomes chaotic when the control parameter has a small change after such a collision. So the resultant SNA typically occurs in the narrow vicinity along the transition boundary between chaotic and periodic phases in the parameter space. There is little discussion whether such a narrow vicinity still remains or can be detected when such a collision happens for a quasiperiodically forced high-dimensional system.

The existence of SNA in the quasiperiodically forced circle map lattices with unidirectional coupling has been investigated [Sosnovtseva *et al.*, 1998], however the unidirectional coupling map lattices are too simple and special for high-dimensional systems. The goal of this paper is to present a general method for the creation of SNA in high-dimensional spatiotemporal systems. Shuai and Wong [1998] pointed out that the low-frequency quasiperiodically driven logistic map can occur as SNA if the dynamics become expanding for long time intervals, repeatedly. Based on this, a general SNA method that is applicable to any chaotic system is presented in Sec. 2, which is applied to high-dimensional systems in the present paper. It shows that the complex behavior in spatiotemporal systems can be due to the strange nonchaotic dynamics, rather than chaotic dynamics. An example of a globally coupled neural network driven by a quasiperiodical signal is presented in Sec. 3. It is the first example of SNA in high-dimensional neural systems. In Sec. 4, a simulation example is studied in detail. Its phase diagram of the example is discussed in Sec. 5. We show that in the parameter space the chaotic phase occurs only within a small region around the origin. A notable result is that more than half of the large nonchaotic region is SNA phase. Another interesting observation is that the chaotic attractors are typically surrounded by SNAs. Conclusions are drawn out in Sec. 6. The relevancy of our results to real neural systems is also discussed in Sec. 6. We suggest that some biological signals that have a strange structure may not be chaotic.

2. Creation of SNA in Chaotic Systems

For an autonomous discrete map $\mathbf{x}(t+1) = \mathbf{G}(\mathbf{x}(t), \xi)$ with the control parameter ξ, the dependent function of the maximum Lyapunov exponent on ξ, i.e. Λ_ξ, can be obtained. Varying ξ, the system can be chaotic or periodic. Suppose when ξ is in region $\mathbf{C}$, the system is chaotic; when ξ is in region $\mathbf{P}$, the system is periodic. Now let the parameter ξ be replaced by a quasiperiodic function given as follows:

$$\xi(t) = A_0 + A_1 \sin(2\pi\omega t) \tag{1}$$

where ω is irrational and small, and $A_1 > 0$. Note the driving period $T = 1/\omega$.

The driving force $\xi(t)$ slowly changes with time in region $\mathbf{R} = (A_0 - A_1,\ A_0 + A_1)$ quasiperiodically. During a short time interval around time t, the force $\xi(t)$ can be approximated by the constant force $F_t = A_0 + A_1 \sin(\theta_t)$ with $\theta_t = 2\pi\omega t$ [Shuai & Durand, 2000]. Thus, whether the dynamics of the system $\mathbf{x}(t+1) = \mathbf{G}(\mathbf{x}(t), \xi(t))$ are expanding or contracting within this short time interval can be estimated by the dynamics of the autonomous system $\mathbf{x}(t+1) = \mathbf{G}(\mathbf{x}(t), F_t)$, which is driven by the constant force F_t. Suppose part of region $\mathbf{R}$ is in $\mathbf{C}$ and the other in $\mathbf{P}$. According to the approximation of constant force, the dynamics of the system are expanding and the trajectory runs into a bursting state when the driving force is in region $\mathbf{C}$; while the dynamics are converging and the trajectory runs into a laminar state when the force is in $\mathbf{P}$. By the name of laminar state, the trajectory stays in a small invariant region. The bursting state means that the trajectory chaotically oscillates in the phase space with a random amplitude.

A low enough frequency ensures that the time interval of expanding dynamics, i.e. the time interval that the force $\xi(t)$ stays in chaotic region $\mathbf{C}$, can be sufficiently long within a driving period. The irrational frequency means that different values of $\xi(t)$ are always provided at different time t. So, with such a time series of $\xi(t)$, different expanding orbits can be obtained under repeatedly appearing long-time expanding dynamics. A strange geometric structure thus occurs. If the converging dynamics are stronger than the expanding dynamics, a negative maximum Lyapunov exponent can be obtained asymptotically. The resultant attractor is nonchaotic but strange. Accordingly, the power spectrum of the trajectory is a broadband spectrum combined with sharp peaks.

The dynamics of the system can be discussed with the finite-time Lyapunov exponent. In particular, the maximum nontrivial Lyapunov exponent $\lambda_\tau(t)$ quantifies the expanding or contracting exponent that the trajectory experiences from time t to $t+\tau$. One can discuss the distribution of $\lambda_\tau(t)$ in two ways. The first way is to consider $\lambda_\tau(t)$ versus the observing time window τ with fixed starting time t_0. Such distribution is discussed for some SNA systems [Prasad *et al.*, 1997]. The finite-time Lyapunov exponent in the SNA systems is characterized with a long-time positive tail. Here we show that the distribution of $\lambda_\tau(t_0)$ has an additional interesting property in SNA system driven by a low-frequency force: typically $\lambda_\tau(t_0)$ become negative periodically with period T in the long-time positive tail. The dynamics of system $\mathbf{x}(t+1) = \mathbf{G}(\mathbf{x}(t), \xi(t))$ in a driving period can be approximated by a number of autonomous systems $\mathbf{x}(t+1) = \mathbf{G}(\mathbf{x}(t), F_t)$. With different driving periods, the same autonomous systems can be applied. Thus, the dynamics of the system with different driving periods are similar. Nonchaotic system guarantees that contracting dynamics should be stronger than expanding dynamics in each driving period. The maximum time interval of continuously positive $\lambda_\tau(t_0)$ must then be smaller than the driving period T, although the maximum time interval having positive $\lambda_\tau(t_0)$ can be large enough.

The second way is to discuss $\lambda_\tau(t)$ versus t with a fixed small τ [Shuai & Wong, 1998]. In this case the observing time window τ is fixed at a small value τ_0. The distribution of $\lambda_{\tau_0}(t)$ versus t for fixed τ_0 can give detailed information about which time intervals the dynamics are expanding, i.e. a strange structure occurs. Suppose that the trajectory runs into a pure expanding region in the long time interval (t_0, t_0+T_A). Then all $\lambda_{\tau_0}(t)$ with $t_1 < t < t_1 + T_A$ are positive. In fact, any small $\tau \ll T_A$ can be applied to discuss the dynamics of the system. Although the exact value of $\lambda_\tau(t)$ varies with the choice of τ, once the trajectory runs into the pure expanding interval (t_0, t_0+T_A), $\lambda_\tau(t)$ and $\lambda_{2\tau}(t)$ typically have the same signs because we have

$$\lambda_{2\tau}(t_0) = \frac{1}{2}(\lambda_\tau(t_0) + \lambda_\tau(t_0+\tau)) \tag{2}$$

Based on the approximation of constant force [Shuai & Durand, 2000], the sign of the finite-time Lyapunov exponent $\lambda_\tau(t)$ of the system $\mathbf{x}(t+1) = \mathbf{G}(\mathbf{x}(t), \xi(t))$ within a small window τ can be estimated by the maximum Lyapunov exponent Λ_F of the autonomous system $\mathbf{x}(t+1) = \mathbf{G}(\mathbf{x}(t), F_t)$.

In short, if a spatiotemporal system is driven by a low-frequency quasiperiodic force to experience expanding dynamics repeatedly with long time intervals, while its asymptotic dynamics are nonchaotic, an SNA occurs. This method can be applied to any chaotic system because one can always find a parameter in such a manner that the system is chaotic or periodic corresponding to different values of the parameter. In fact, the dimensionality of the mapping $\mathbf{G}$ is neither mentioned nor needed here for the creation of SNA. In the present paper we focus on the high-dimensional neural system.

3. SNA in Neural Model

As an application, a globally coupled neural network is discussed in the paper. The model consists of N analog neurons $\{S_i(t)\}$, $i = 1, \ldots, N$, with $-1 \le S_i \le 1$, where every neuron S_i is connected to all other neurons S_j by random couplings $\{J_{ij}\}$. The following parallel dynamics are used for updating of the neurons:

$$S_i(t+1) = g(h_i(t)), \quad i = 1, \ldots, N. \tag{3}$$

The sigmoidal function which is a typical transfer function in neural models is used here

$$g(x) = \tanh(\alpha x) \tag{4}$$

with $\alpha > 0$. The internal field h_i of the neuron S_i is given by

$$h_i(t) = \sum_{j=1}^{N} J_{ij} S_j(t) + \xi_i(t) \tag{5}$$

with $\xi_i(t)$ as the external signal. Usually, the external stimulus only affects part of the neural networks. Therefore, assuming that only the first M ($M \le N$) neurons are stimulated by the input signal:

$$\begin{aligned} \xi_i(t) &= \xi(t), \quad i = 1, \ldots, M. \\ \xi_i(t) &= 0, \qquad i = M+1, \ldots, N. \end{aligned} \tag{6}$$

Without any stimulus, the neural dynamics are typically chaotic because of the asymmetric coupling [Molgedey *et al.*, 1992]. Now consider a constant driving signal with $\xi(t) = F_{\mathrm{Const}}$. Equations (3)–(6) show that the trajectory of the system driven by $-F$ with the initial conditions $\{S_i(0)\}$ is the same as that driven by F with $\{-S_i(0)\}$. So the dynamical properties, including the Lyapunov exponents, are the same for the system driven by $-F$ or by F.

If $M = N$, a large stimulus can always drive the neural network to be periodic. This is because, with a large stimulus, the internal fields of all the neurons are mainly determined by the stimulus and so $S_i(t) \to 1$ for all neurons with any different initial conditions. Thus a periodic attractor is obtained. Our simulation results also show that for a large enough M, a large stimulus can drive the neural network to be periodic. The observation that the stimulus F_0 can drive the network to be periodic just indicates a fact that, if the states of the first M neurons approach 1, the neural network intrinsically becomes periodic. A larger stimulus F_0 only means that the states of the first M neurons are closer to 1. So, if a large F_0 can drive the neural network to be periodic, any larger stimulus F ($> F_0$) can drive the network to be periodic. There is a threshold stimulus F_{Tr} that the chaotic state only appears in the region of $\mathbf{C} = (-F_{\mathrm{Tr}}, F_{\mathrm{Tr}})$. The fact that a F large only means close to 1 for the states of the first M neurons also suggests that the Lyapunov exponents Λ_F are almost constant with large F for periodic attractors.

Now there is a chaotic region $\mathbf{C}$ with $|F| < |F_{\mathrm{Tr}}|$ and a periodic region $\mathbf{P}$ with $|F| > |F_{\mathrm{Tr}}|$. One can then use the approach discussed in Sec. 2 to generate SNA. To do it, the input signal ξ in Eq. (1) is applied. It is easy to see that the dynamical trajectory of the system for $\xi(t) = A_0 + A_1 \sin(\theta(t))$ with initial conditions ($\{S_i(0)\}$, θ_0) is the same as that for: $\xi(t) = A_0 - A_1 \sin(\theta(t))$ with ($\{S_i(0)\}$, $\theta_0 + \pi$); $\xi(t) = -A_0 - A_1 \sin(\theta(t))$ with initial conditions ($\{-S_i(0)\}$, θ_0); or $\xi(t) = -A_0 + A_1 \sin(\theta(t))$ with ($\{-S_i(0)\}$, $\theta_0 + \pi$). Thus, the attractors of the system are identical for the external signals of $\pm A_0 \pm A_1 \sin(\theta(t))$. In other words, the dynamical properties, e.g. Lyapunov exponents and fractal dimension, are symmetric about the A_0-axis and A_1-axis in $A_0 - A_1$ plane. So in the following, we only discuss the situation of the force in the first quadrant in A_0–A_1 plane, i.e. A_0, $A_1 > 0$.

With a low frequency, the slowly changed stimulus $\xi(t)$ can be approximated by the constant input $F_t = A_0 + A_1 \sin(\theta(t))$ within a small time interval. If $A_0 + A_1 < F_{\mathrm{Tr}}$, i.e. the stimulus is always within the chaotic region $\mathbf{C}$, the dynamics of the networks are typically expanding, resulting in a chaotic attractor. If $A_0 - A_1 > F_{\mathrm{Tr}}$, i.e. the stimulus is always out of chaotic region $\mathbf{C}$, the dynamics of the networks are typically contracting, resulting in a torus. If $A_0 + A_1 > F_{\mathrm{Tr}} > A_0 - A_1$, the stimulus $\xi(t)$ goes in and out of the chaotic region $\mathbf{C}$ twice during each driving period. So its dynamics become expanding or contracting repeatedly. In this region, a strange but nonchaotic attractor may be generated. In the following, a simulation example is discussed in detail to confirm this discussion.

4. Simulation Results of SNA

In the simulation, let $N = 100$ and $M = 20$. A set of randomly selected coupling weights $\{J_{ij}\}$ uniformly distributed from -1 to 1 is used in the simulation. Without any extended signal, the neural dynamics are chaotic with the maximum Lyapunov exponent $\Lambda = 0.095$. Figure 1(a) gives the dependence of the Lyapunov exponent Λ_F as a function of positive scalar stimulus F. The chaotic attractor

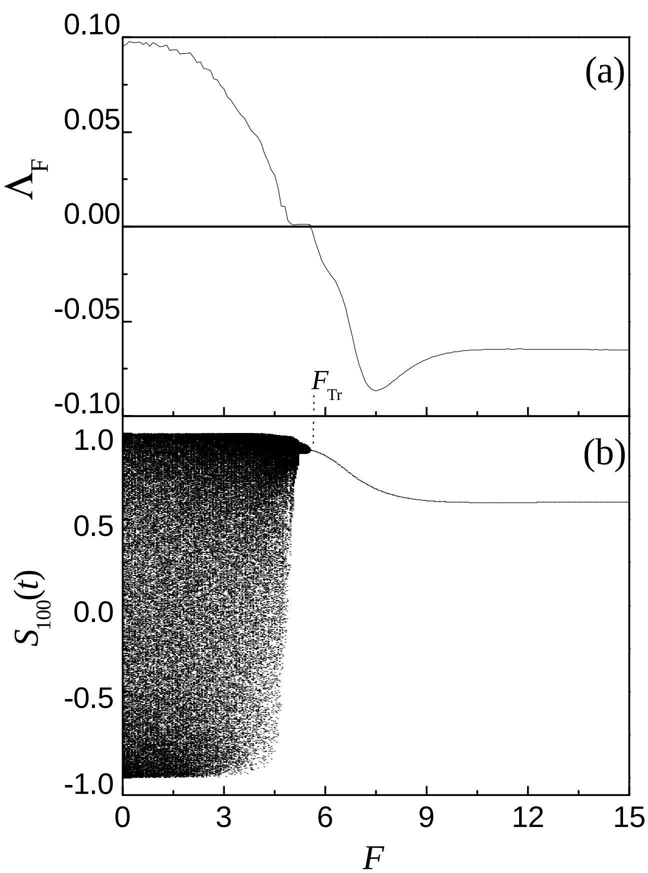

Fig. 1. (a) Lyapunov exponent Λ_F and (b) the bifurcation diagram of neuron 100 versus the constant signal F for the neural system driven by F. Here F is from 0 to 15.

undergoes a transition to periodic when $F = F_{\mathrm{Tr}} \approx 5.56$. The chaotic states only appear in a finite region $\mathbf{C} = (-F_{\mathrm{Tr}}, F_{\mathrm{Tr}})$ of the parameter space. As expected, Λ_F is almost constant for $F > 10$. Figure 1(b) gives its bifurcation diagram of neuron 100 with F from 0 to 15.

In this paper, a quasiperiodical stimulus $\xi(t)$ with $\omega = 0.001 \cdot \sqrt{5}$, i.e. the driving period $T \approx 448$ is used to stimulate the network. Simulation results show the following: (1) for $A_0 = 9$ and $A_1 = 2$, a torus attractor **A** is obtained with the nontrivial maximum Lyapunov exponent $\Lambda = -0.074$; (2) for $A_0 = 2$ and $A_1 = 9$, a nonchaotic attractor **B** is obtained with $\Lambda = -0.085$; (3) for $A_0 = 2$ and $A_1 = 8$, a chaotic attractor **C** is obtained with $\Lambda = 0.005$; and (4) for $A_0 = 2$ and $A_1 = 2$, a chaotic attractor **D** is obtained with $\Lambda = 0.078$. The spatiotemporal patterns of these four attractors are shown in

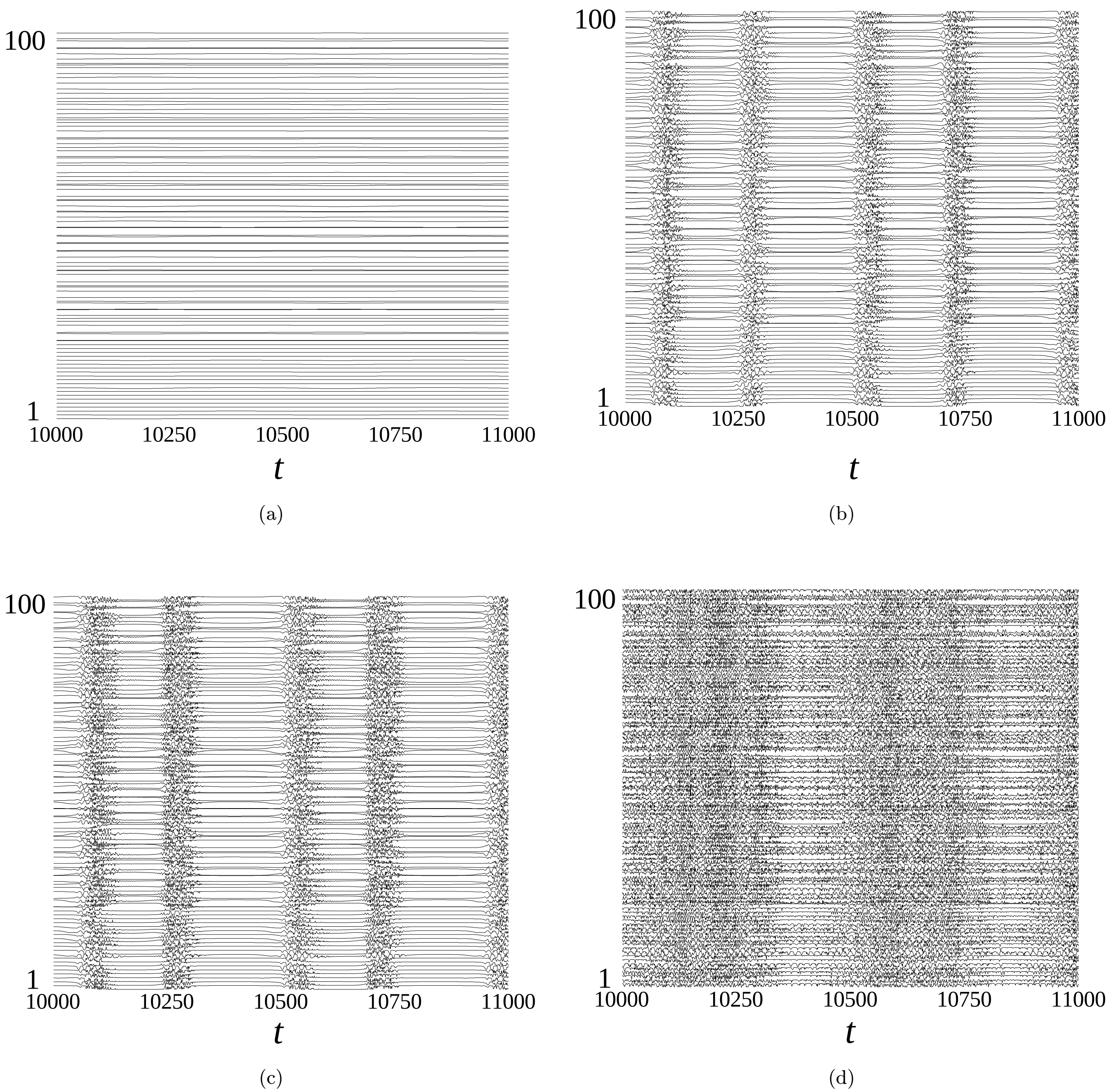

Fig. 2. Oscillating states of the 100 neurons via time from 10 000 to 11 000 of the attractor (a) **A**, (b) **B**, (c) **C** and (d) **D**.

Fig. 2 which shows that both the nonchaotic attractor **B** and the chaotic attractor **C** possess the intermittency behavior between laminar and bursting states. Their geometric structures are quite similar. These observations suggest that attractor **B** is an SNA.

SNAs also exhibit a singular continuous power spectrum lying among the sharp peaks. In Figs. 3(A)–3(D), the power spectra versus frequency plots are given for the four trajectories of the 100th neuron which is not driven directly by the sine signal. The spectral shape of attractors **B** and **C** are quite similar as shown in Figs. 3(B) and 3(C). There is a broadband spectrum with the addition of some large peaks as expected from the combined behavior of periodic [Fig. 3(A)] and chaotic systems [Fig. 3(D)]. The broad band spectrum for attractor **B** implies that there is a finite-time expanding behavior in a chaotic manner that yields a strange structure, rather than a torus.

The finite-time nontrivial maximum Lyapunov exponents $\lambda_{\tau_0}(t)$ versus time t with the observing time window $\tau_0 = 10$ are plotted in Fig. 4 for the four attractors. For attractor **A**, $\lambda_{\tau_0}(t)$ is typically negative, indicating an torus obtained. For attractor **D**, $\lambda_{\tau_0}(t)$ is typically positive. Therefore a chaotic attractor occurs. For attractors **B** and **C**, driven by the quasiperiodical force, $\lambda_{\tau_0}(t)$ oscillates between negative and positive values. In particular, their signs change from the negative to the positive twice in a driving period. The intermittency between laminar and burst behavior is then a characteristic dynamic of such attractors.

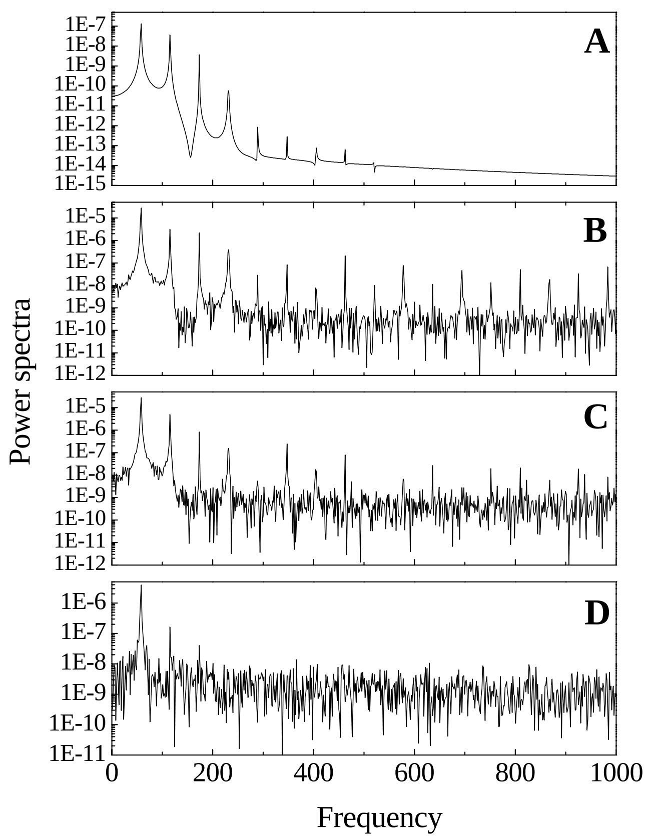

Fig. 3. Power spectra versus frequency in the region of $(0, 1000)$ for the trajectories of neuron 100 of the four attractors. Here 16384 points are calculated for each curve. The frequency is in arbitrary unit.

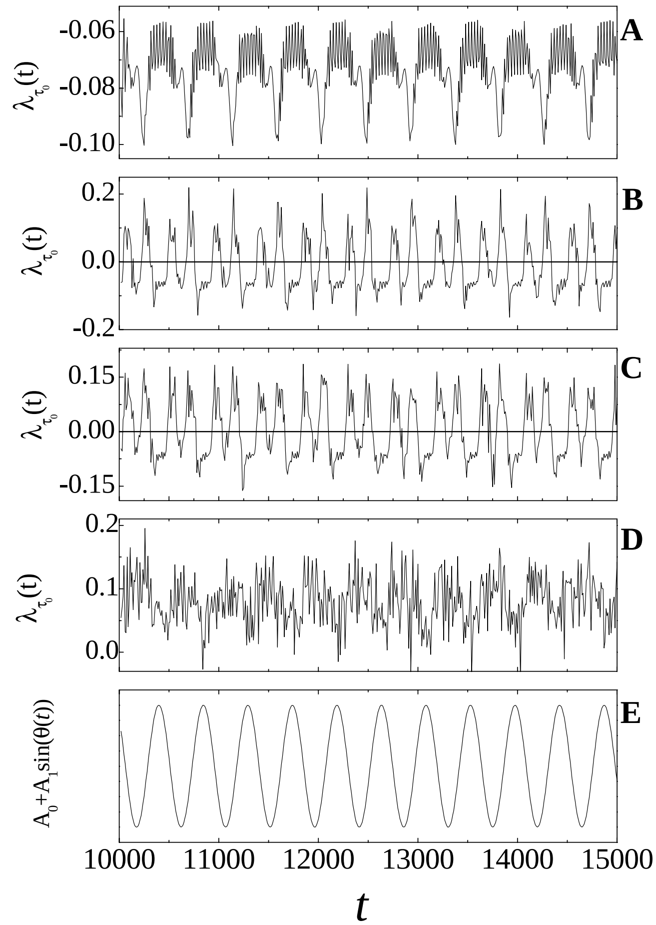

Fig. 4. Finite-time Lyapunov exponents $\lambda_{\tau_0}(t)$ versus time t from 10 000 to 15 000 with observing time window $\tau_0 = 10$ for attractors **A**, **B**, **C** and **D**. Here (E) shows the applied quasiperiodically driving force as a function of time.

As shown in Fig. 1, the dynamics of the networks are expanding only when F falls into the chaotic region $\mathbf{C} = (-5.56, 5.56)$. For attractor **A**, stimulus $9 + 2\sin(2\pi\omega t)$ is always out of region **C**, so $\lambda_{\tau_0}(t)$ is typically negative and its trajectory is a laminar state. For attractor **D**, stimulus $2 + 2\sin(2\pi\omega t)$ is always within region **C** and so $\lambda_{\tau_0}(t)$ is typically positive and the trajectory is

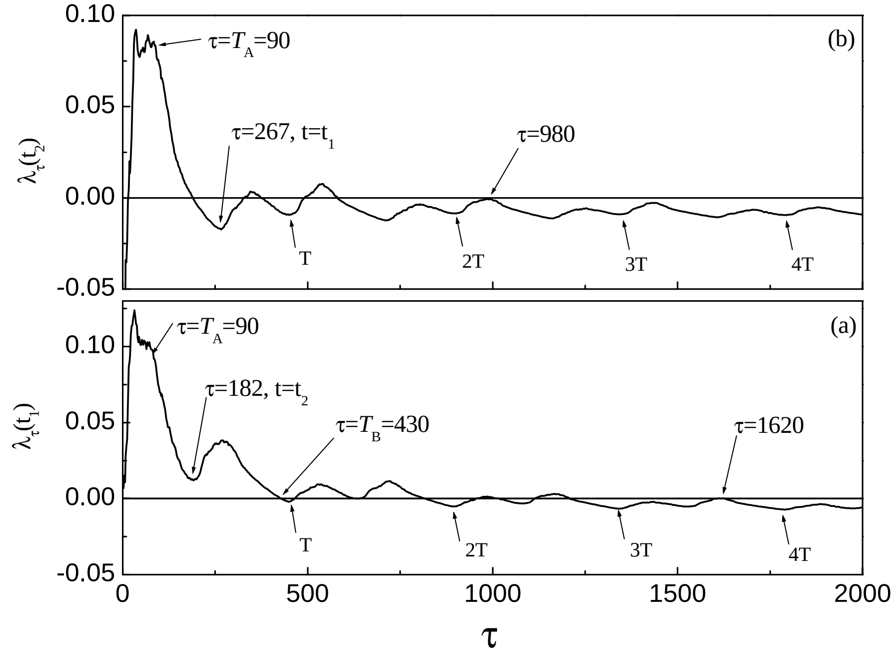

Fig. 5. Finite-time Lyapunov exponents $\lambda_\tau(t)$ versus observing time window τ from 0 to 2000 for attractors **B** with the starting time (a) $t_1 = 10\,033$ and (b) $t_2 = 10\,215$.

always bursting. For attractor **B** or **C**, stimulus $2 + 9\,\sin(2\pi\omega t)$ or $2 + 8\,\sin(2\pi\omega t)$ goes in and out of the chaotic region **C** twice during each driving period, so $\lambda_{\tau_0}(t)$ changes its sign twice in a driving period. Simulation results also confirm that the changes of the sign occur when $F(t) \approx \pm 5.56$. Here $\tau_0 = 10$. The subsequent time interval of expanding dynamics is about $T_A = 10\tau_0 = 100$ for attractor **B**, as shown in Fig. 4(b). Within the repeatedly expanding time intervals, a strange geometric structure is yielded for nonchaotic attractor **B**.

Figure 5 gives the plot of $\lambda_\tau(t)$ versus observing time window τ for attractor **B** with fixed starting time $t_1 = 10\,033$ and $t_2 = 10\,215$ which are in the same period of the driving force. At time t_1, t_2, the driving forces are about 5.56 and -5.56, respectively, and the trajectory is being driven to the expanding region. In this case, the maximum time interval for a positive finite-time Lyapunov exponent can be obtained. Figure 5(a) shows that the exponents have large positive values as long as $\tau = T_A = 90$, within which the dynamics are expanding. Then for $90 < \tau < 182$, the trajectory is driven to the contracting region although $\lambda_\tau(t)$ only decreases to a small positive level. When $\tau = 182$ (i.e. $t = t_2$), the dynamics become expanding again and then $\lambda_\tau(t_1)$ reaches another positive peak. Exponent $\lambda_\tau(t)$ remains positive until $\tau = T_B = 430$. However, $\lambda_\tau(t_1)$ is positive for τ as long as 1620. Simulation results show that $\lambda_\tau(t_1)$ asymptotically approach to -0.085 in an oscillating manner with longer τ. In Fig. 5(b), $\lambda_\tau(t)$ can be positive when $\tau = 980$. As discussed above, $\lambda_\tau(t)$ is always negative when $\tau = nT$, which means that the contracting dynamics are stronger than the expanding dynamics in each driving period and therefore its asymptotic Lyapunov exponent is negative. Simulations show that similar results can be observed with any starting time $t = t_{1,2} + nT$.

5. Phase Diagram

For a dynamic system, one can distinguish its chaotic phase from nonchaotic phase easily by checking if the value of its maximum nontrivial Lyapunov exponent Λ is positive. A nonchaotic attractor is by definition an SNA if it has a strange geometric structure. In particular, we observe the geometric structure of the nonchaotic attractor in the S–θ phase space. The phase space of a neuron is $(-1,\,1)$. For a typical SNA, its trajectory repeatedly bursts in a chaotic manner to a large phase space (whose scale is more than 1) with a long time period. In other words, a long positive finite time Lyapunov exponent can be observed for an SNA. Simulation results of phase diagram are given in Fig. 6 in A_0–A_1 plane with $0 < A_0$, $A_1 < 25$ for the present example.

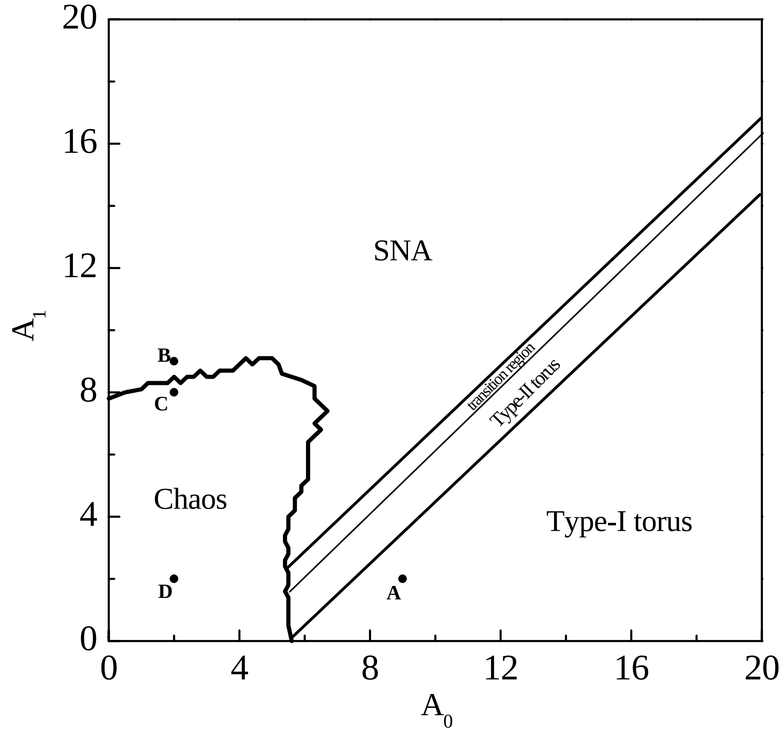

Fig. 6. Phase diagram of the present neural networks in the first quadrant in A_0–A_1 plane. The four points corresponding to attractors **A**, **B**, **C** and **D** are also shown in the parameter space.

As shown in Fig. 6, the chaotic phase only occurs in a finite region near the origin in A_0–A_1 plane. This can be comprehended based on the approximation of constant driving force which suggests that the Lyapunov exponent Λ of the system can be estimated from the average of a set of Lyapunov exponents Λ_F of the autonomous systems [Shuai & Durand, 2000]. If the values of A_0 or A_1 of the driving force are quite larger than $F_{\rm Tr}$, most of the applied constant forces F_t must be larger than $F_{\rm Tr}$ and so most of the finite-time Lyapunov exponents are negative. As a result, a negative Lyapunov exponent Λ can be expected, indicating a nonchaotic attractor.

In Fig. 6, two types of torus (type-I and II torus) are distinguished. The type-I torus is in the region with $A_1 < A_0 - F_{\rm Tr} = A_0 - 5.56$. Because the instant driving force is always in the periodic region, the dynamics of a type-I torus are typically contracting and its finite-time Lyapunov exponent is always negative. The dynamics of a type-II torus sometimes can become expanding, i.e. its finite-time Lyapunov exponent can be positive. The expanding time interval can sometimes be as long as 50. But the corresponding time intervals are so small that the resultant trajectory does not show a large bursting state. Simulation results show that in the nonchaotic region between $A_1 < A_0 - 4$ and $A_1 > A_0 - 5.56$ type-II torus is observed. By further increasing the parameter A_1, the scales of the bursting states are enlarged gradually and the attractor translates from torus to SNA after a transition region.

SNAs can be found typically in the nonchaotic region of $A_1 > A_0 - 3.2$. According to the approximation of constant force, in order to obtain a piece of expanding dynamics, the region of driving force $\xi(t)$, i.e. $(A_0 - A_1, A_0 + A_1)$, must overlap the chaotic region $\mathbf{C} = (-F_{\rm Tr}, F_{\rm Tr})$. So, $A_0 - A_1 < F_{\rm Tr}$. Furthermore, to generate a strange structure, expanding dynamics must occur for long time intervals. Long-time expanding dynamics guarantee the trajectory can burst in a chaotic manner to a large phase space. Simulation results show that if each time interval of expanding dynamics is more than 80, a largely bursting state can occur. Thus, $A_1 > A_0 - 3.2$ can be expected. Because the dynamic properties (Lyapunov exponents and fractal dimension) are symmetric about the A_0-axis and A_1-axis in the A_0–A_1 plane, the phase diagram of the present neural network in $A_0 - A_1$ plane can be easily obtained. The chaotic phase occurs only within a small region around the origin in A_0–A_1 plane. The nonchaotic phase exists in a large region, more than half of which is the SNA phase. This is the first example to observe an SNA region that is larger than chaotic region or torus region. Another interesting observation is that, except near the A_0-axis, the chaotic phase is typically surrounded by SNAs.

6. Discussion and Conclusion

A general method is presented in this paper for the creation of SNA in spatiotemporal systems that can be chaotic or periodic depending on a constant driving force. When a low-frequency quasiperiodic force is applied, the dynamics of the system can be driven to oscillate between expanding and converging states. Long-time expanding dynamics lead to a strange attractor. If the contracting dynamics dominate the expanding dynamics, the resultant attractor is strange but nonchaotic. With this method SNAs can occur in a large area in parameter space. For such an SNA, the time interval of continuously positive finite-time Lyapunov exponent must be smaller than the period of the driving force, although it has a long-time positive tail.

A simple neural network driven by a low-frequency quasiperiodic signal is discussed as an example. Driven by the low-frequency quasiperiodic stimulus, the chaotic phase of the neural network appears only in a small region around the origin in A_0–A_1 plane and the SNA can occur in a large area of the nonchaotic region. Because this simple neural model contains some important features of the real neural system, it is capable of reproducing some basic behavior of real neural networks. It has been difficult to prove whether a biological signal is chaotic [Freeman, 1987; Lutzenberger *et al.*, 1995]. However, our results indicate that some complex biological signals that have a strange structure may not be chaotic. SNAs may be observed in some real neural systems. This new classification could have important consequences in the analysis of the biological signals, particularly for complex biological signals such as those seen in epilepsy.

Strange nonchaotic dynamics could be applicable to the analysis of biological neural signals generated by biological networks such as the electroencephalogram (EEG). It has been shown that the human EEG has a fractal dimension [Lutzenberger *et al.*, 1995]. The EEG has been studied in the view of low-dimensional chaotic dynamics [Babloyantz *et al.*, 1985; Freeman, 1987]. However, a number of recent studies analyzing the Lyapunov exponent [Theiler, 1995] and surrogate data [Rombouts *et al.*, 1995; Palus, 1996; Stam *et al.*, 1997] suggest that the EEG is unlikely to be chaotic. It is also shown that a positive Lyapunov exponent could be calculated with time series of SNA [Shuai *et al.*, 2001]. Different mechanisms such as a noisy limit cycle, a noisy two-frequency oscillation and quasiperiodic oscillations, as well as the linearly filtered noise, have been proposed to explain the EEG dynamics [Theiler, 1995; Rombouts *et al.*, 1995; Palus, 1996; Stam *et al.*, 1997]. It has been shown that different neuronal population in the cortex can oscillate at different frequencies [Gray *et al.*, 1989]. If the quasiperiodic dynamics can occur and the EEG is not chaotic, it is then a reasonable hypothesis that EEG dynamics may be due to strange nonchaotic behavior.

Acknowledgments

We would like to thank W. C. Stacey for helpful discussion. This work is supported by NSF grant no. IBN 93-19599 and a Whitaker Development Award to the Department of Biomedical Engineering.

References

Babloyantz, A., Salazar, J. M. & Nicolis, C. [1985] "Evidence of chaotic dynamics of brain activity during the sleep cycle," *Phys. Lett.* **A111**, 152–156.

Brown, R. & Chua, L. O. [1998] "Clarifying chaos II: Bernoulli chaos, zero Lyapunov exponents and strange attractors," *Int. J. Bifurcation and Chaos* **8**, 1–32.

Ding, M., Grebogi, C. & Ott, E. [1989] "Evolution of attractors in quasiperiodically forced systems: From quasiperiodic to strange nonchastic to chastic," *Phys. Rev.* **A39**, 2593–2598.

Ditto, W. L., Spano, M. L., Savage, H. T., Rauseo, S. N., Heagy, J. & Ott, E. [1990] "Experimental observation of a strange nonchaotic attractor," *Phys. Rev. Lett.* **65**, 533–536.

Freeman, W. J. [1987] "Simulation of chaotic EEG patterns with a dynamic model of the olfactory system," *Biol. Cybern.* **56**, 139–150.

Gray, C. M., Konig, P., Engel, A. K. & Singer, W. [1989] "Oscillatory responses in cat visual cortex exhibit inter columnar synchronization which reflects global stimulus properties," *Nature* **338**, 334–337.

Grebogi, C., Ott, E., Pelikan, S. & Yorke, J. A. [1984]

"Strange attractors that are not chaotic," *Physica* **D13**, 261–268.

Heagy, J. F. & Hammel, S. M. "The birth of strange nonchaotic attractors," *Physica* **D70**, 140–153.

Hopfield, J. J. [1982] "Neural networks and physical systems with emergent collective computational abilities," *Proc. Natl. Acad. Sci. USA* **79**, 2554–2558.

Kaneko, K. [1990] "Globally coupled chaos violates the law of large numbers but not the central limit theorem," *Phys. Rev. Lett.* **65**, 1391–1394.

Lutzenberger, W., Preissl, H. & Pulvermuller, F. [1995] "Fractal dimension of electroencephalographic time series and underlying brain processes," *Biol. Cybern.* **73**, 477–482.

Molgedey, L., Schuchhardt, J. & Schuster, H. G. [1992] "Suppressing chaos in neural networks by noise," *Phys. Rev. Lett.* **69**, 3717–3719.

Nishikava, T. & Kaneko, K. [1996] "Fractalization of a torus as a strange nonchaotic attractor," *Phys. Rev.* **E54**, 6114–6124.

Palus, M. [1996] "Nonlinearity in normal human EEG: Cycles, temporal asymmetry, nonstationarity and randomness, not chaos," *Biol. Cybern.* **75**, 389–396.

Prasad, A., Mehra, V. & Ramaswamy, R. [1997] "Intermittency routes to strange nonchaotic attractors," *Phys. Rev. Lett.* **79**, 4127–4130.

Rombouts, S. A. R. B., Keunen, R. W. M. & Stam, C. J. [1995] "Investigation of nonlinear structure in multichannel EEG," *Phys. Lett.* **A202**, 352–358.

Shuai, J. W. & Wong, K. W. [1998] "Nonchaotic attractors with highly fluctuating finite time Lyapunov exponents," *Phys. Rev.* **E57**, 5332–5336.

Shuai, J. W. & Wong, K. W. [1999] "Simple approach to the creation of a strange nonchaotic attractor in any chaotic system," *Phys. Rev.* **E59**, 5338–5343.

Shuai, J. W. & Durand, D. M. [2000] "Strange nonchaotic attractor in low frequency quasiperiodically driven systems," *Int. J. Bifurcation and Chaos* **10**, 2269–2276.

Shuai, J. W., Lian, J., Hahn, P. J. & Durand, D. M. [2001] "Positive Lyapunov exponents calculated from time-series of strange nonchaotic attractors," *Phys. Rev.* **E64**, 26220-1–26220-5.

Sosnovtseva, O., Vadivasova, T. E. & Anishchenko, V. S. [1998] "Evolution of complex oscillations in a quasiperiodically forced chain," *Phys. Rev.* **E57**, 282–287.

Stam, C. J., van Woerkom, T. C. A. M. & Keunen, R. W. M. [1997] "Nonlinear analysis of the electroencephalogram in Creutzfeldt–Jakob disease," *Biol. Cybern.* **77**, 247–256.

Theiler, J. [1995] "On the evidence for low dimensional chaos in an epileptic electroencephalogram," *Phys. Lett.* **A196**, 335–341.

Vergni, D., Falcioni, M. & Vulpiani, A. [1997] "Spatial complex behavior in nonchaotic flow systems," *Phys. Rev.* **E56**, 6170–6172.

Yalcinkaya, T. & Lai, Y. C. [1996] "Blowout bifurcation routs to strange nonchaotic attractors," *Phys. Rev. Lett.* **77**, 5039–5042.